ORIGINAL ARTICLE

CrossMark

^{68}Ga-PSMA PET/CT for monitoring response to ^{177}Lu-PSMA-617 radioligand therapy in patients with metastatic castration-resistant prostate cancer

Alexander Heinzel[1,2] · Dima Boghos[1] · Felix M. Mottaghy[3] · Florian Gaertner[4] · Markus Essler[4] · Dirk von Mallek[1] · Hojjat Ahmadzadehfar[4]

Abstract

Purpose To evaluate the use of ^{68}Ga-PSMA PET/CT for monitoring response to ^{177}Lu-617 PSMA radioligand therapy in patients with metastatic castrate-resistant prostate cancer (mCRPC).

Methods Patients from the University Hospital Bonn and the University Hospital Aachen were retrospectively reviewed for this study. We included 48 patients with mCRPC who were treated with ^{177}Lu-PSMA-617 and whose records included ^{68}Ga-PSMA PET/CT imaging before the first and after the third or fourth treatment cycle. A treatment response based on ^{68}Ga-PSMA PET/CT was defined according to a modified version of the PERCIST criteria. A decline in PSA level of ≥50% was considered the reference standard. The sensitivity, specificity, positive and negative predictive values, and ROC curves were calculated, and patient survival times in relation to the PET results were also analysed.

Results ^{68}Ga-PSMA PET/CT had a sensitivity of about 85% and a specificity of between 55% and 65%. The negative and positive predictive values ranged between 70% and 78%. The fitted ROC area was 0.70. The survival time was about 19.6 months in patients with a treatment response, while nonresponders had a survival time of about 15.9 months. However, this difference between the groups was not statistically significant.

Conclusion Our results indicate that ^{68}Ga-PSMA PET/CT could be a useful tool for the evaluation of response to ^{177}Lu-PSMA-617 radioligand therapy within a theranostic framework.

Keywords Prostate cancer · ^{177}Lu-PSMA-617 · ^{68}Ga-PSMA PET/CT · Response monitoring

Introduction

Prostate cancer is the most common cancer in men in the US and Europe, as well as one of the most common

✉ Alexander Heinzel
aheinzel@ukaachen.de

1 Department of Nuclear Medicine, University Hospital RWTH Aachen, Pauwelsstrasse 30, 52074 Aachen, Germany

2 Institute for Neuroscience and Medicine (INM-4), Research Centre Jülich, Jülich, Germany

3 Department of Radiology and Nuclear Medicine, Maastricht University Medical Center, Maastricht, The Netherlands

4 Department of Nuclear Medicine, University Hospital Bonn, Bonn, Germany

malignancies worldwide and the fifth leading cause of cancer mortality in men [1]. A recent approach to the treatment and diagnosis of prostate cancer specifically targets the unique membrane-bound glycoprotein prostate-specific membrane antigen (PSMA). PSMA is overexpressed in prostate cancer, and is upregulated in poorly differentiated, metastatic and hormone-refractory carcinomas [2, 3].

Since prostate cancer is usually radiosensitive, systemic treatment using radiolabelled PSMA ligands that are internalized into cancer cells can be expected to effectively deliver high doses. The PSMA-617 ligand shows favourable dosimetry with high receptor-binding affinity, efficient internalization into prostate cancer cells and low kidney uptake [4]. Consistent with these properties, radioligand therapy with ^{177}Lu-PSMA-617 has shown promise as a targeted therapy in patients with metastatic castration-resistant prostate cancer (mCRPC) [5–7]. Similarly, in clinical studies PET/CT imaging with ^{68}Ga-labelled PSMA ligands has been used successfully for primary staging and for image-

guided radiotherapy and surgery in patients with recurrent prostate cancer and advanced-stage metastatic prostate cancer [4, 8].

Based on these results, PSMA is an ideal membrane-bound structure for both imaging and targeted therapy for prostate cancer, thereby enabling a theranostic approach (i.e. the same molecule is used for both in vivo imaging and therapy) [9]. A crucial aspect of the theranostic approach is the ability to monitor treatment response. Based on the evidence discussed above, many centres already use PET/CT imaging with ^{68}Ga-PSMA. This procedure is also recommended by the German consensus statement and the European guidelines [10, 11]. However, direct empirical evidence is so far lacking. Therefore, we designed a two-centre retrospective study on the use of PET/CT with ^{68}Ga-PSMA for monitoring response to treatment with ^{177}Lu-PSMA-617 in patients with mCRPC.

Typically, response to treatment is assessed using the Response Evaluation Criteria in Solid Tumors (RECIST) and the updated RECIST 1.1 [12]. However, according to the original RECIST, bone metastases are considered unmeasurable. RECIST 1.1 includes bone metastases as target lesions, but only if they have associated soft tissue components. Thus, most bone metastases derived from prostate cancer are still excluded from these quantitative response assessments [13]. To apply objective response criteria in our study, we used the modified version of RECIST, the PET Response Criteria in Solid Tumors (PERCIST) [14].

The cornerstone measurement for monitoring treatment response in patients with mCRPC is prostate-specific antigen (PSA) [15]. However, the results of some studies have led to the questioning of the association between changes in PSA levels and treatment response. For example, an initial increase in PSA levels following treatment with ^{223}Ra-dichloride does not necessarily prove disease progression, but may either be a nonresponse or represent a prognostically favourable flare [16]. Therefore, new more effective biomarkers such as circulating tumour cells and circulating DNA are being developed [16, 17]. Therefore, in this study the relationships between PET tracer uptake and changes in PSA levels and patient survival time were investigated.

Materials and methods

Subjects

Patients who had received ^{68}Ga-PSMA PET/CT from November 2014 to January 2018 for the monitoring of treatment with ^{177}Lu-PSMA-617 were retrospectively recruited from the departments of nuclear medicine of the university hospitals of Bonn and Aachen.

We included patients with mCRPC who had been treated with ^{177}Lu-PSMA-617 and in whom ^{68}Ga-PSMA PET/CT

imaging had been performed before the first and after the third or fourth treatment cycle. In every patient initially four treatment cycles were planned, but some patients did not receive the fourth cycle. In these patients response to treatment was evaluated on the PET/CT scan after the third cycle. The PET scans had to be performed between 4 and 12 weeks after the respective treatment cycle. All patients had disease progression despite first-line or second-line chemotherapy (docetaxel or cabazitaxel) or were ineligible for chemotherapy or ^{223}Ra-dichloride treatment. In addition, only patients who had been treated with at least one of the new-generation antihormonal drugs (abiraterone or enzalutamide) before the ^{177}Lu-PSMA-617 treatment were considered. The time between the ^{68}Ga-PSMA PET/CT scan and the PSA measurements had to be 4 weeks or less. Patients whose pretherapy and posttherapy PET/CT scans were performed on different scanners were excluded.

^{177}Lu-PSMA-617 therapy

^{177}Lu-PSMA-617 treatment was performed in both centres according to the German consensus statement [11]. The treatment protocol has been described in detail elsewhere [6]. Briefly, in both centres the radioligand was produced in-house using a PSMA-617 precursor from ABX GmbH (Radeberg, Germany) and ^{177}Lu from ITG Isotope Technologies and IDB Holland BV. For each cycle, a standard activity of 6 GBq of ^{177}Lu-PSMA-617 was administered. After treatment administration, whole-body scintigraphic imaging was performed to document the uptake of ^{177}Lu-PSMA-617 in the tumour lesions. High uptake was shown in metastatic lesions, in accordance with the pretherapy ^{68}Ga-PSMA PET/CT images.

^{68}Ga-PSMA PET/CT scans

The ^{68}Ga-PSMA-HBED-CC tracer for the PET/CT scans was produced by the in-house radiopharmacy using a previously reported method [18]. The patients received an intravenous injection of approximately 2 MBq/kg body weight of ^{68}Ga-PSMA 45 min before the start of the PET/CT scan. The patients were scanned in caudocranial orientation with their arms raised. Attenuation correction was performed using the CT data.

The scans performed at the Department of Nuclear Medicine, University Hospital Bonn, were acquired in 3D mode using a Biograph 2 PET/CT scanner (Siemens Medical Solutions, Erlangen, Germany). The emission time was 4 min per bed position. The PET images were reconstructed iteratively (attenuation-weighted OSEM, four iterations, eight subsets) and included scatter, random and decay corrections. The images were smoothed using a 5-mm gaussian filter. The scans performed at the Department of Nuclear Medicine, University Hospital Aachen, were acquired in 3D

mode using a Philips Gemini TF 16 (Philips Medical Systems, Best, The Netherlands). The emission time was 1.5 min per bed position over 9 to 11 bed positions. Slices of 4 mm thickness (voxel size 4 mm × 4 mm) were reconstructed using the BLOB-OS-TF algorithm (three iterations, 33 subsets).

Analysis of the ^{68}Ga-PSMA PET/CT scans

In accordance with previous studies, we defined any focal uptake of ^{68}Ga-PSMA ligand higher than that of the surrounding background and not associated with physiological uptake as suspicious for malignancy [19, 20]. PSMA uptake in the lacrimal, parotid and submandibular glands, as well as in the liver, spleen, small intestine, colon and kidney was considered as physiological. PSMA uptake was assessed by measuring the peak standardized uptake value (SUVpeak) according to a modified version of the PERCIST [14]. Thus, volumes of interest of diameter 1.2 cm centred around the voxel with the highest activity in the tumour foci were used. Diverging from these recommendations, we did not calculate the SUV normalized to lean body mass (SUL), since we sought to use an easily reproducible measure, and lean body weight is rarely calculated in the clinical setting using PSMA PET/CT. Instead, we calculated the difference in SUVpeak (ΔSUV) between the pretherapy scan and the scan after the third or fourth treatment cycle (i.e. if a scan was performed after the fourth treatment cycle, we used that scan; otherwise, we used the scan after the third treatment cycle). A minimum reduction in the target measurable tumour SUVpeak of 30% was considered a treatment response, in the absence of new lesions. New lesions were defined according to PERCIST, i.e. a lesion was considered new when it was first visualized, irrespective of any retrospective review of earlier scans [21].

The measurable tumour SUVpeak was calculated using two methods:

1. As the difference between the pretherapy and posttherapy scans in the highest SUV in any lesion (Δ highest SUV).
2. As the difference between the pretherapy and posttherapy scans in the mean SUV of the lesions with the highest uptake of all tissues with metastases, calculated as the mean of the SUV of the tumour lesion with the highest uptake in the lymph nodes and highest SUV in other tissues if they contain metastases (Δ mean SUV).

Clinical parameters

With regard to PSA, we defined treatment response according to the Prostate Cancer Clinical Trials Working Group 3 criteria, i.e. a decline in PSA level of ≥50% compared to baseline was considered a response [15]. Patient survival time was determined starting from the pretherapy PET/CT scan until patient death or until the last patient contact if the patient was still alive (censored).

Data analysis

We defined treatment response according to ^{68}Ga-PSMA PET/CT as a Δ highest SUV (Δ mean SUV) of ≥30%. Thus, a Δ highest SUV (Δ mean SUV) of ≥30% combined with a ΔPSA of ≥50% was considered a true-positive response, a Δ highest SUV (Δ mean SUV) of ≥30% combined with a ΔPSA of <50% was considered a false-positive response, a Δ highest SUV (Δ mean SUV) of <30% combined with a ΔPSA of <50% was considered a true-negative response, and a Δ highest SUV (Δ mean SUV) of <30% combined with a ΔPSA of ≥50% was considered a false-negative response. Based on these values, we calculated the sensitivity, specificity, positive predictive value and negative predictive value for the use of ^{68}Ga-PSMA PET/CT for the assessment of response to ^{177}Lu-PSMA-617 radioligand therapy. This was done separately for Δ highest SUV and Δ mean SUV. These assessments were based on a blinded reading of the scans.

Since the analysis was based on data from two institutions the use of SUVpeak alone might have led to some challenges. Therefore, we additionally calculated the lesion to liver SUV ratio in all patients. To that end we measured the SUVpeak of the liver (SUVliver) by applying a volume of interest of diameter 5 cm centred around the voxel with the highest activity.

For the statistical analyses, we used SPSS® 25 (IBM® SPSS® Statistics, IBM Inc. Armonk, NY, USA). We calculated the means and medians for the survival times, plotted the Kaplan-Meier curves and used the log rank (Mantel-Cox) test to evaluate the equality of the survival distributions between the different groups. The patients were divided into two groups, those with a treatment response (PETresp group) and those with no treatment response (PETn-resp group). To calculate the receiver operating characteristic (ROC) curves, we used a web-based calculator for ROC curves (http://www.jrocfit.org).

Results

We initially identified 80 patients for possible inclusion in this study. However, 32 patients were excluded due to a lack of data (i.e. no posttherapy PET/CT or measurement of PSA levels later than 4 weeks after the PET/CT scan). Thus, 48 patients were included in the analysis. Of these patients, 60% had received previous treatment with docetaxel, 20% with cabazitaxel, 65% with abiraterone, 71% with enzalutamide, 40% with both abiraterone and enzalutamide, 40% with ^{223}Ra-dichloride and 50% with external radiation therapy. Details related to the treatment responses are shown in Supplementary Table 1.

Table 1 Sensitivity, specificity, negative predictive value and positive predictive value of ^{68}Ga-PSMA PET/CT in detecting a decline in PSA level of >50% after treatment with ^{177}Lu-PSMA-6171

	Sensitivity	Specificity	Negative predictive value	Positive predictive value
Δ highest SUV	0.84	0.65	0.76	0.75
Δ mean SUV	0.88	0.55	0.78	0.70

Δ highest SUV difference in highest SUV in any lesion between the pretherapy and posttherapy scans, *Δ mean SUV* difference between the pretherapy and posttherapy scans in the mean SUV of the lesions with the highest uptake of all tissues with metastases, calculated as the mean of the SUV of the lesion with highest uptake in bones and the SUV of the lesion with the highest uptake in lymph nodes

The statistical measures of the performance of ^{68}Ga-PSMA PET/CT in detecting a decline in PSA level of >50% are shown in Table 1. For both methods (Δ highest SUV and Δ mean SUV), there was a sensitivity of about 85% and a specificity of between 55% and 65%. The negative and positive predictive values ranged between 70% and 78%. The ROC curves for both methods were almost identical, with only slightly different fitted ROC areas: 0.706 for Δ mean SUV and 0.709 for Δ highest SUV. Figure 1 shows the ROC curves for Δ highest SUV.

The performance values using the lesion to liver SUV ratio are shown in Table 2. They were similar to those obtained using SUVpeak alone.

Due to the high sensitivity of ^{68}Ga-PSMA PET/CT, false-negative results, i.e. no treatment response according to PET criteria but a decrease in PSA, level, are considered rare. However, it is more common for the ^{68}Ga-PSMA PET/CT scan result to be false-positive, i.e. a decrease in Δ highest SUV and Δ mean SUV, but no corresponding decrease in PSA level of ≥50%. Two typical examples are shown in Figs. 2 and 3. Figure 2 shows PET images in a patient with diffuse skeletal metastases. Since the applied response criteria referred to the voxel with the highest activity, diffuse skeletal metastases were disregarded, even though they may have represented the largest part of the total tumour volume. Figure 3 shows

PET images in a patient with a mixed response, emphasizing the difficulty in taking nontarget lesions into account. In this patient, the mediastinal lymph node metastases showed high ^{68}Ga-PSMA PET uptake, representing the lesion with the highest activity in the pretherapy images. In the posttherapy images, there was increased uptake in a bone lesion in the right ilium that was still much lower than the uptake in the mediastinal lymph node metastases in the pretherapy images. Thus, the images were evaluated as a treatment response, since the increase was only related to a nontarget lesion on the pretherapy images and not to the voxel with the highest activity.

We also evaluated the relationship between treatment response on ^{68}Ga-PSMA PET/CT and survival times. The results are presented in Tables 3 and 4, which show estimated mean survival times between 20.0 and 19.6 months in the PETresp group and between 15.9 and 15.0 months in the PETn-resp group, suggesting a difference in survival time between the groups. The corresponding Kaplan-Meier curves are shown in Fig. 4. However, the difference in Δ highest SUV between the groups was not statistically significant (log-rank Mantel-Cox test chi-squared 0.266, with df 1; $p = 0.606$), and the difference in Δ mean SUV between the groups was also not statistically significant (log-rank Mantel-Cox test chi-squared 0.811, with df 1; $p = 0.368$).

Fig. 1 ROC curve for Δ mean SUV with 95% confidence intervals (*green and red curves*; *y axis* true-positive fraction, *x axis* false-positive fraction). Fitted ROC area 0.709. The ROC curve for Δ mean SUV was almost identical and is therefore not shown
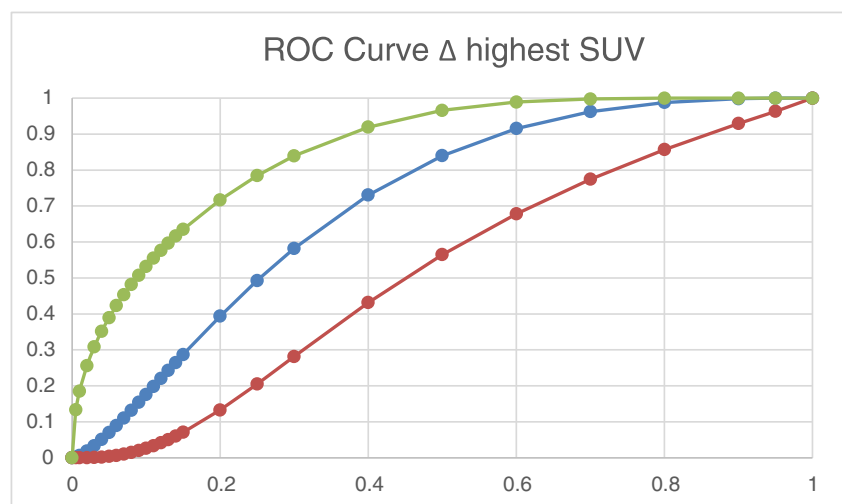

ROC Curve Δ highest SUV

Table 2 Sensitivity, specificity, negative predictive value and positive predictive value of ^{68}Ga-PSMA PET/CT in detecting a decline in PSA level of >50% after treatment with ^{177}Lu-PSMA-6171

	Sensitivity	Specificity	Negative predictive value	Positive predictive value
Ratio Δ high	0.85	0.64	0.73	0.78
Ratio Δ mean	0.84	0.56	0.69	0.75

Ratio Δ high difference between the pretherapy and posttherapy scans in highest lesion to liver SUV ratio in any lesion, *ratio Δ mean* difference between the pretherapy and posttherapy scans in the mean SUV of the lesions with the highest uptake of all tissues with metastases/liver SUV, calculated as the mean of the SUV of the lesion with highest uptake in the bones/liver SUV and the SUV of the lesion with highest uptake in lymph nodes/liver SUV

Discussion

There is a growing amount of evidence that ^{177}Lu-PSMA-617 treatment of mCRPC patients is associated with encouraging response rates and a low toxicity profile [22, 23]. Thus, in a theranostic framework, ^{68}Ga-PSMA PET/CT is the logical imaging modality of choice for evaluating treatment response. Detection of lymph node or bone metastases from prostate cancer is sometimes difficult with morphological imaging methods such as CT and MRI [24, 25]. In contrast, the use of ^{68}Ga-PSMA PET/CT has spread rapidly and this modality is considered a significant step forward in prostate cancer imaging [26–30].

Based on the reference standard of a decrease in PSA level of >50%, our results showed that PET/CT with ^{68}Ga -PSMA has a sensitivity of about 85% and a specificity of between 55% and 65%, with negative and positive predictive values ranging between 70% and 78%. Thus, this approach has a satisfactory sensitivity, but a low specificity with the risk of false-positive results. Several factors may explain the low specificity. First, the measurements of secreted protease PSA and the cell surface PSMA are based on different biological processes that may be subject to different regulatory influences. For example, data in the literature indicate that PSMA overexpression is related to high intratumour angiogenesis activity, while this may not be the case for high PSA levels [31]. Also, studies have shown that while androgen deprivation treatment can lead to decreases in PSA levels, it can also cause increases in PSMA expression and the related ^{68}Ga-PSMA uptake [22, 28]. Although PSMA expression and serum PSA levels are often strongly correlated, these biomarkers address slightly different prostate cancer properties. Thus, their measurements may differ depending on the biological properties of the individual tumour, leading to divergent serum PSA levels and ^{68}Ga-PSMA uptake results.

Second, if our treatment evaluation criteria were to be applied to patients with diffuse skeletal metastases that show a homogeneous ^{68}Ga-PSMA uptake in the whole skeleton, the results may be misleading. In some patients, diffuse skeletal metastases show a few hot spots that reduce after treatment, even though the overall diffuse uptake is unchanged or even increased (however, not enough to count as new target lesions). In such patients, we found false-positive results.

Fig. 2 PET images in patient 11 show a clear decrease in tracer uptake in lesions with the highest activity including lesions in the right rib, lumbar vertebral column and left pelvis (*red arrowheads*; Δ highest SUV 61%, Δ mean SUV 61%). However, the diffuse skeletal uptake seems to be unchanged or even slightly increased. There was a corresponding increase in PSA level of 69%. Thus the PET findings were considered false-positive
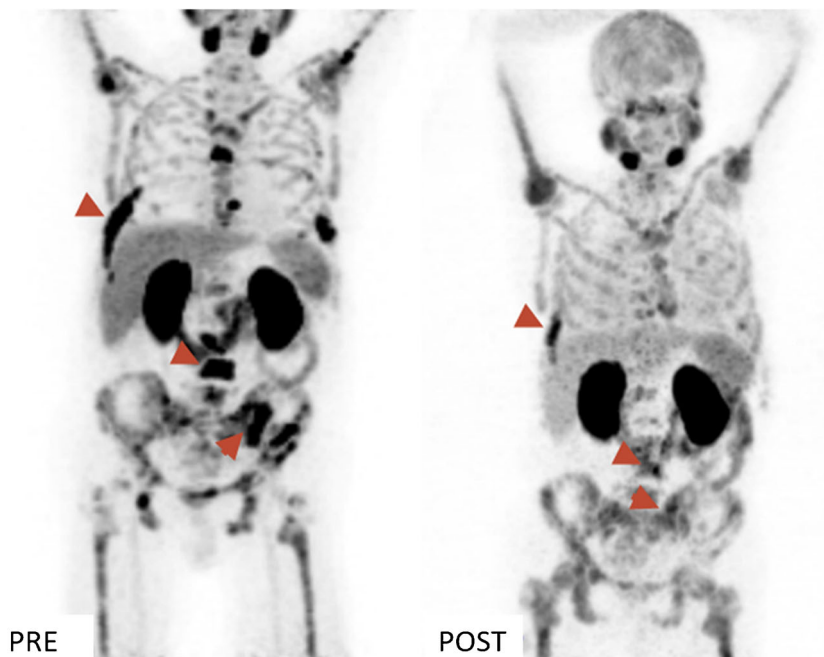
PRE

POST

Fig. 3 PET images in patient 28 show a mixed response. Highest activity is seen in a lesion in the mediastinal lymph nodes (*blue arrow*) in the pretherapy image (*PRE*). Tracer uptake is clearly decreased (*blue arrow*) in the posttherapy image (*POST*). However, tracer uptake is increased in a bone lesion in the right ilium (*red arrowheads*). According to our criteria, the lesion with the highest activity in each image was measured (i.e. in the mediastinal lymph nodes in the pretherapy image and in the right ilium in the posttherapy image) resulting in a Δ highest SUV of 52% and a Δ mean SUV of 60% leading to evaluation as a treatment response. However, there was an increase in PSA level of 56%. Thus, the PET findings were considered false-positive
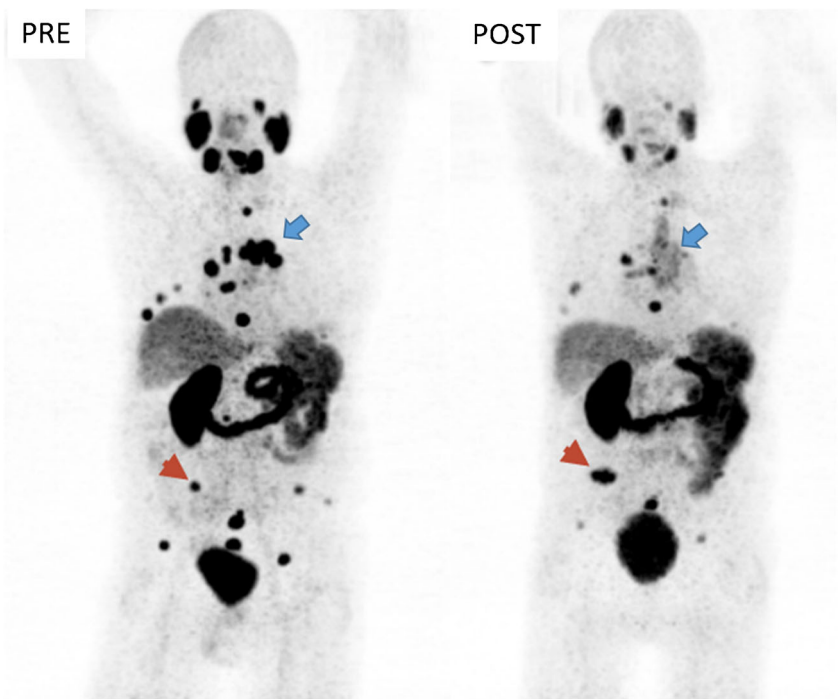
Thus, different criteria may be needed to correctly evaluate treatment response in these patients. For example, in these patients, the mean ^{68}Ga-PSMA uptake of the total tumour volume of the whole skeleton may be considered the target lesion [32]. Further studies are needed to specifically address this problem. Third, there is the unresolved issue of unequivocal progression in the PERCIST framework [21], where the unequivocal progression of nontarget lesions is not precisely defined. Our data show some patients with a mixed response, emphasizing the difficulty in taking nontarget lesions into account. In such patients, the use of different and stricter criteria might be necessary.

In this study, we used two different methods to evaluate treatment response (Δ highest SUV and Δ mean SUV). Both methods are closely related to the PERCIST framework. However, diverging from the PERCIST guidelines, we did not calculate the lean SUVpeak, since this is currently a difficult parameter to calculate in the clinical setting. The

possibility that calculation of lean SUVpeak might have led to better results cannot be excluded. However, it was our goal to design an easily applicable method for evaluating the treatment response. In addition, a recent study has demonstrated that ^{18}F-DCFPyL PET images, and perhaps PSMA-targeted PET images in general, show less variability when SUV is normalized to body mass than when SUV is normalized to lean body mass, favouring adoption of normalization to body mass [33].

The Δ highest SUV closely corresponds to the PERCIST framework. We included Δ mean SUV because there are indications that the effect of treatment with ^{177}Lu-PSMA-617 may be different for metastases in different tissues due to differences in uptake and radiation sensitivity. For example, Kulkarni et al. [5] found that lymph node metastases respond better to ^{177}Lu-PSMA-617 treatment than bone metastases. The Δ mean SUV accounts for all tissues with metastases, thereby controlling for these factors. However,

Table 3 Survival times in relation to treatment response according to Δ highest SUV

Response group	Survival (months)					
	Mean			Median		
	Value	Standard error	95% confidence interval	Value	Standard error	95% confidence interval
PETresp	19.586	1.831	15.997–23.174	17.000	2.490	12.120–21.880
PETn-resp	15.926	2.172	11.669–20.183	11.000	3.182	4.763–17.237
Overall	19.098	1.627	15.910–22.287	16.000	2.549	11.004–20.996

PETresp Δ highest SUV indicates treatment response, *PETn-resp* Δ highest SUV indicates no treatment response

Table 4 Survival times in relation to treatment response according to Δ mean SUV

Response group	Survival (months)						
	Mean			Median			
	Value	Standard error	95% confidence interval	Value	Standard error	95% confidence interval	
PETresp	19.955	1.777	16.472–23.439	19.000	2.599	13.907–24.093	
PETn-resp	15.000	2.302	10.488–19.512	10.000	2.000	6.080–13.920	
Overall	19.098	1.627	15.910–22.287	16.000	2.549	11.004–20.996	

PETresp Δ mean SUV indicates treatment response, *PETn-resp* Δ mean SUV indicates no treatment response

Fig. 4 Kaplan-Meier survival curves for responders (*blue*) and nonresponders (*red*) determined according to Δ high SUV (**a**) and Δ mean SUV (**b**) on ^{68}Ga-PSMA PET/CT
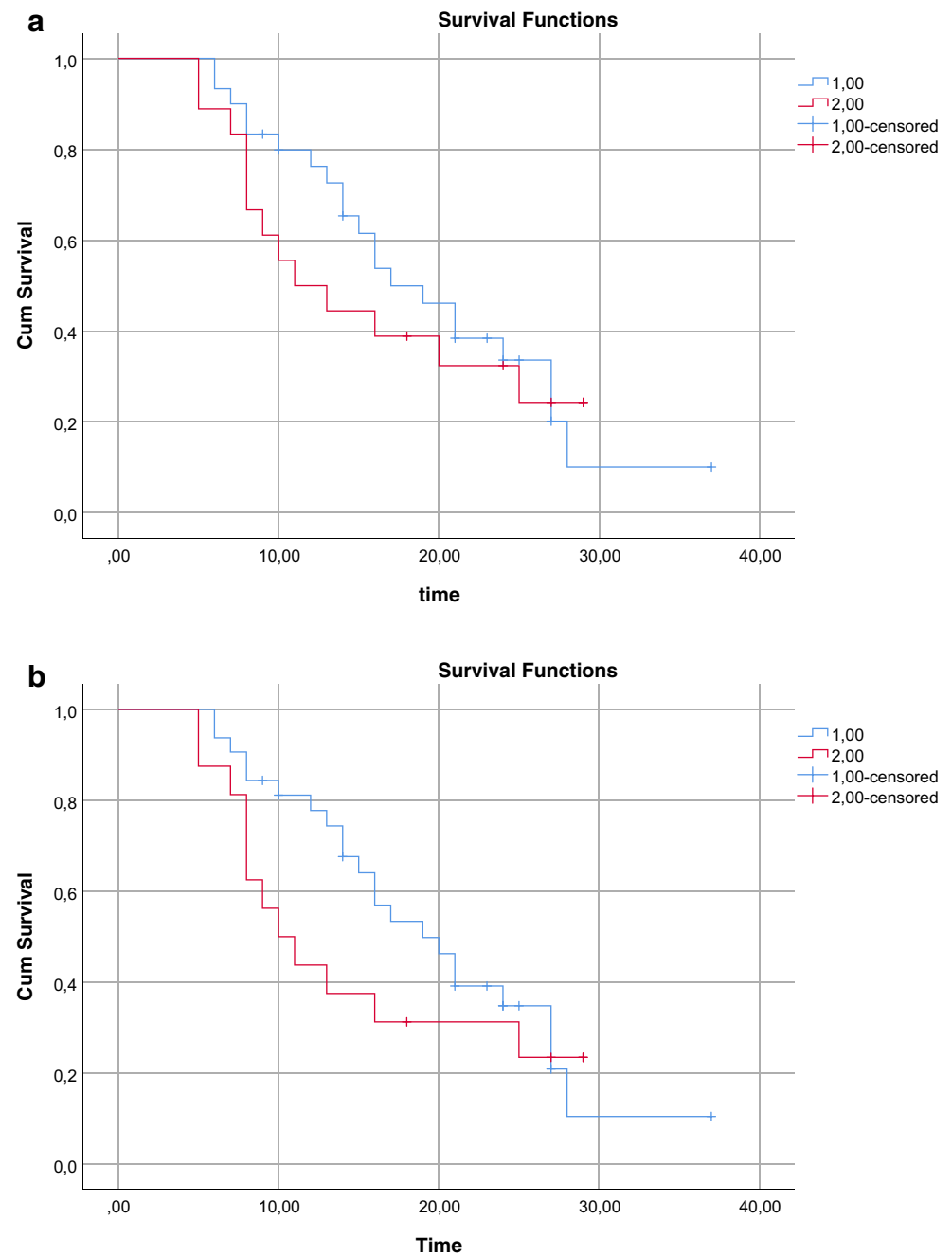
both methods showed almost identical performance parameters with identical ROC curves and areas under the curve. Thus, the simpler method (i.e. the Δ highest SUV) may be applied in the clinical setting.

The survival analysis showed that patients with a treatment response on ^{68}Ga-PSMA PET/CT had a survival time of about 19.6 months, while nonresponders had a survival time of about 15.9 months. However, the statistical analysis using the log rank test showed that this difference was not statistically significant. This was also illustrated by the Kaplan-Meier curves that tended to show a difference between the groups up to 28 months that was no longer present in the later time course. This might have been due to the small sample size, with 29% of patients (14 of 48) censored. A larger sample size with fewer censored patients might reveal statistically significant differences between groups. Another problem to be addressed is nonspecific PSMA binding. Several studies have shown non-malignant aetiologies of tracer uptake, e.g. in ganglia and thyroid, as well as uptake in other tumours due to neovascularization [34, 35]. In analysing our data we carefully tried to avoid the known pitfalls but, ultimately, the possibility that these factors influenced the results cannot be excluded.

In addition to ^{68}Ga-labelled PSMA ligands, ^{18}F-labelled compounds such as ^{18}F-DCFPyL and ^{18}F-PSMA-1007 have been introduced [36, 37]. Preliminary data for ^{18}F-PSMA-1007 suggest superior sensitivity for small lesions. Thus, the use of this tracer might improve sensitivity for the monitoring of ^{177}Lu-PSMA-617 radioligand therapy.

Conclusion

^{68}Ga-PSMA PET/CT appears to be a promising tool for monitoring ^{177}Lu-PSMA-617 radioligand therapy within a theranostic framework. However, the problem of false-positive results should be addressed in further studies, for example, by improving the methods for evaluating ^{68}Ga-PSMA uptake. These aspects will be addressed in prospective studies with larger sample sizes.

Compliance with ethical standards

Conflicts of interest None.

Ethical approval This study was approved by the Institutional Review Board of the University Hospital Aachen. Given the type of study (a retrospective analysis), the need for written informed consent was waived. All procedures were performed in accordance with the ethical standards of the institutional and/or national research committees and with the principles of the 1964 Declaration of Helsinki and its later amendments or comparable ethical standards.

Publisher's note Springer Nature remains neutral with regard to jurisdictional claims in published maps and institutional affiliations.

References

1. Wong MC, Goggins WB, Wang HH, Fung FD, Leung C, Wong SY, et al. Global incidence and mortality for prostate cancer: analysis of temporal patterns and trends in 36 countries. Eur Urol. 2016;70: 862–74. https://doi.org/10.1016/j.eururo.2016.05.043.

2. Benesova M, Schafer M, Bauder-Wust U, Afshar-Oromieh A, Kratochwil C, Mier W, et al. Preclinical evaluation of a tailor-made DOTA-conjugated PSMA inhibitor with optimized linker moiety for imaging and endoradiotherapy of prostate cancer. J Nucl Med. 2015;56:914–20. https://doi.org/10.2967/jnumed.114.147413.

3. Ghosh A, Heston WD. Tumor target prostate specific membrane antigen (PSMA) and its regulation in prostate cancer. J Cell Biochem. 2004;91:528–39. https://doi.org/10.1002/jcb.10661.

4. Kratochwil C, Afshar-Oromieh A, Kopka K, Haberkorn U, Giesel FL. Current status of prostate-specific membrane antigen targeting in nuclear medicine: clinical translation of chelator containing prostate-specific membrane antigen ligands into diagnostics and therapy for prostate cancer. Semin Nucl Med. 2016;46:405–18. https://doi.org/10.1053/j.semnuclmed.2016.04.004.

5. Kulkarni HR, Singh A, Schuchardt C, Niepsch K, Sayeg M, Leshch Y, et al. PSMA-based radioligand therapy for metastatic castration-resistant prostate cancer: the Bad Berka experience since 2013. J Nucl Med. 2016;57:97S–104S. https://doi.org/10.2967/jnumed.115.170167.

6. Rahbar K, Ahmadzadehfar H, Kratochwil C, Haberkorn U, Schafers M, Essler M, et al. German multicenter study investigating 177Lu-PSMA-617 radioligand therapy in advanced prostate cancer patients. J Nucl Med. 2017;58:85–90. https://doi.org/10.2967/jnumed.116.183194.

7. Rahbar K, Schmidt M, Heinzel A, Eppard E, Bode A, Yordanova A, et al. Response and tolerability of a single dose of 177Lu-PSMA-617 in patients with metastatic castration-resistant prostate cancer: a multicenter retrospective analysis. J Nucl Med. 2016;57: 1334–8. https://doi.org/10.2967/jnumed.116.173757.

8. Lutje S, Heskamp S, Cornelissen AS, Poeppel TD, van den Broek SA, Rosenbaum-Krumme S, et al. PSMA ligands for radionuclide imaging and therapy of prostate cancer: clinical status. Theranostics. 2015;5:1388–401. https://doi.org/10.7150/thno.13348.

9. Haberkorn U, Kopka K, Giesel F, Kratochwil C. Future trends in prostate cancer theranostics with PSMA ligands. Clin Transl Imaging. 2016;4:487–9.

10. Fendler WP, Eiber M, Beheshti M, Bomanji J, Ceci F, Cho S, et al. (68)Ga-PSMA PET/CT: joint EANM and SNMMI procedure guideline for prostate cancer imaging: version 1.0. Eur J Nucl Med Mol Imaging. 2017;44:1014–24. https://doi.org/10.1007/s00259-017-3670-z.

11. Fendler WP, Kratochwil C, Ahmadzadehfar H, Rahbar K, Baum RP, Schmidt M, et al. 177Lu-PSMA-617 therapy, dosimetry and follow-up in patients with metastatic castration-resistant prostate cancer. Nuklearmedizin. 2016;55:123–8.

12. Eisenhauer EA, Therasse P, Bogaerts J, Schwartz LH, Sargent D, Ford R, et al. New response evaluation criteria in solid tumours: revised RECIST guideline (version 1.1). Eur J Cancer. 2009;45: 228–47. https://doi.org/10.1016/j.ejca.2008.10.026.

13. Wallace T, Torre T, Grob M, Yu J, Avital I, Brücher B, et al. Current approaches, challenges and future directions for monitoring treatment response in prostate cancer. J Cancer. 2014;5:3–24. https://doi.org/10.7150/jca.7709.

14. Wahl RL, Jacene H, Kasamon Y, Lodge MA. From RECIST to PERCIST: evolving considerations for PET response criteria in solid tumors. J Nucl Med. 2009;50(Suppl 1):122S–50S. https://doi.org/10.2967/jnumed.108.057307.

15. Scher HI, Morris MJ, Stadler WM, Higano C, Basch E, Fizazi K, et al. Trial design and objectives for castration-resistant prostate cancer: updated recommendations from the Prostate Cancer Clinical Trials Working Group 3. J Clin Oncol. 2016;34:1402–18. https://doi.org/10.1200/jco.2015.64.2702.

16. Castello A, Macapinlac HA, Lopci E, Santos EB. Prostate-specific antigen flare induced by (223)RaCl2 in patients with metastatic castration-resistant prostate cancer. Eur J Nucl Med Mol Imaging. 2018;45:2256–63. https://doi.org/10.1007/s00259-018-4051-y.

17. Scher HI, Jia X, de Bono JS, Fleisher M, Pienta KJ, Raghavan D, et al. Circulating tumour cells as prognostic markers in progressive, castration-resistant prostate cancer: a reanalysis of IMMC38 trial data. Lancet Oncol. 2009;10:233–9. https://doi.org/10.1016/s1470-2045(08)70340-1.

18. Eder M, Schafer M, Bauder-Wust U, Hull WE, Wangler C, Mier W, et al. 68Ga-complex lipophilicity and the targeting property of a urea-based PSMA inhibitor for PET imaging. Bioconjug Chem. 2012;23:688–97. https://doi.org/10.1021/bc200279b.

19. Rauscher I, Maurer T, Fendler WP, Sommer WH, Schwaiger M, Eiber M. (68)Ga-PSMA ligand PET/CT in patients with prostate cancer: how we review and report. Cancer Imaging. 2016;16:14. https://doi.org/10.1186/s40644-016-0072-6.

20. Uprimny C, Kroiss AS, Fritz J, Decristoforo C, Kendler D, von Guggenberg E, et al. Early PET imaging with ^{68}Ga-PSMA-11 increases the detection rate of local recurrence in prostate cancer patients with biochemical recurrence. Eur J Nucl Med Mol Imaging. 2017;44:1647–55. https://doi.org/10.1007/s00259-017-3743-z.

21. O JH, Lodge MA, Wahl RL. Practical PERCIST: a simplified guide to PET response criteria in solid tumors 1.0. Radiology. 2016;280:576–84. https://doi.org/10.1148/radiol.2016142043.

22. Hofman MS, Violet J, Hicks RJ, Ferdinandus J, Thang SP, Akhurst T, et al. [(177)Lu]-PSMA-617 radionuclide treatment in patients with metastatic castration-resistant prostate cancer (LuPSMA trial): a single-centre, single-arm, phase 2 study. Lancet Oncol. 2018;19:825–33. https://doi.org/10.1016/s1470-2045(18)30198-0.

23. Rahbar K, Afshar-Oromieh A, Jadvar H, Ahmadzadehfar H. PSMA theranostics: current status and future directions. Mol Imaging. 2018;17:1536012118776068. https://doi.org/10.1177/1536012118776068.

24. Evangelista L, Bertoldo F, Boccardo F, Conti G, Menchi I, Mungai F, et al. Diagnostic imaging to detect and evaluate response to therapy in bone metastases from prostate cancer: current modalities and new horizons. Eur J Nucl Med Mol Imaging. 2016;43:1546–62. https://doi.org/10.1007/s00259-016-3350-4.

25. Hovels AM, Heesakkers RA, Adang EM, Jager GJ, Strum S, Hoogeveen YL, et al. The diagnostic accuracy of CT and MRI in the staging of pelvic lymph nodes in patients with prostate cancer: a meta-analysis. Clin Radiol. 2008;63:387–95. https://doi.org/10.1016/j.crad.2007.05.022.

26. Afshar-Oromieh A, Avtzi E, Giesel FL, Holland-Letz T, Linhart HG, Eder M, et al. The diagnostic value of PET/CT imaging with the (68)Ga-labelled PSMA ligand HBED-CC in the diagnosis of recurrent prostate cancer. Eur J Nucl Med Mol Imaging. 2015;42:197–209. https://doi.org/10.1007/s00259-014-2949-6.

27. Afshar-Oromieh A, Haberkorn U, Eder M, Eisenhut M, Zechmann CM. [68Ga]Gallium-labelled PSMA ligand as superior PET tracer for the diagnosis of prostate cancer: comparison with 18F-FECH. Eur J Nucl Med Mol Imaging. 2012;39:1085–6. https://doi.org/10.1007/s00259-012-2069-0.

28. Afshar-Oromieh A, Malcher A, Eder M, Eisenhut M, Linhart HG, Hadaschik BA, et al. PET imaging with a [68Ga]gallium-labelled PSMA ligand for the diagnosis of prostate cancer: biodistribution in humans and first evaluation of tumour lesions. Eur J Nucl Med Mol Imaging. 2013;40:486–95. https://doi.org/10.1007/s00259-012-2298-2.

29. Afshar-Oromieh A, Zechmann CM, Malcher A, Eder M, Eisenhut M, Linhart HG, et al. Comparison of PET imaging with a (68)Ga-labelled PSMA ligand and (18)F-choline-based PET/CT for the diagnosis of recurrent prostate cancer. Eur J Nucl Med Mol Imaging. 2014;41:11–20. https://doi.org/10.1007/s00259-013-2525-5.

30. Caroli P, Sandler I, Matteucci F, De Giorgi U, Uccelli L, Celli M, et al. (68)Ga-PSMA PET/CT in patients with recurrent prostate cancer after radical treatment: prospective results in 314 patients. Eur J Nucl Med Mol Imaging. 2018;45:2035–44. https://doi.org/10.1007/s00259-018-4067-3.

31. Mottaghy FM, Heinzel A, Verburg FA. Molecular imaging using PSMA PET/CT versus multiparametric MRI for initial staging of prostate cancer: comparing apples with oranges? Eur J Nucl Med Mol Imaging. 2016;43:1397–9. https://doi.org/10.1007/s00259-016-3389-2.

32. Filss C, Heinzel A, Miiller B, Vogg ATJ, Langen KJ, Mottaghy FM. Relevant tumor sink effect in prostate cancer patients receiving 177Lu-PSMA-617 radioligand therapy. Nuklearmedizin. 2018;57:19–25. https://doi.org/10.3413/Nukmed-0937-17-10.

33. Li X, Rowe SP, Leal JP, Gorin MA, Allaf ME, Ross AE, et al. Semiquantitative parameters in PSMA-targeted PET imaging with (18)F-DCFPyL: variability in normal-organ uptake. J Nucl Med. 2017;58:942–6. https://doi.org/10.2967/jnumed.116.179739.

34. Keidar Z, Gill R, Goshen E, Israel O, Davidson T, Morgulis M, et al. 68Ga-PSMA PET/CT in prostate cancer patients – patterns of disease, benign findings and pitfalls. Cancer Imaging. 2018;18:39. https://doi.org/10.1186/s40644-018-0175-3.

35. Krohn T, Verburg FA, Pufe T, Neuhuber W, Vogg A, Heinzel A, et al. [(68)Ga]PSMA-HBED uptake mimicking lymph node metastasis in coeliac ganglia: an important pitfall in clinical practice. Eur J Nucl Med Mol Imaging. 2015;42:210–4. https://doi.org/10.1007/s00259-014-2915-3.

36. Dietlein M, Kobe C, Kuhnert G, Stockter S, Fischer T, Schomacker K, et al. Comparison of [(18)F]DCFPyL and [(68)Ga]Ga-PSMA-HBED-CC for PSMA-PET imaging in patients with relapsed prostate cancer. Mol Imaging Biol. 2015;17:575–84. https://doi.org/10.1007/s11307-015-0866-0.

37. Giesel FL, Hadaschik B, Cardinale J, Radtke J, Vinsensia M, Lehnert W, et al. F-18 labelled PSMA-1007: biodistribution, radiation dosimetry and histopathological validation of tumor lesions in prostate cancer patients. Eur J Nucl Med Mol Imaging. 2017;44:678–88. https://doi.org/10.1007/s00259-016-3573-4.